THE JOURNAL OF BIOLOGICAL CHEMISTRY VOL. 285, NO. 21, pp. 16258–16266, May 21, 2010

Growth and Tumor Suppressor NORE1A Is a Regulatory Node between Ras Signaling and Microtubule Nucleation*[S]

Received for publication, November 2, 2009, and in revised form, March 23, 2010 Published, JBC Papers in Press, March 25, 2010, DOI 10.1074/jbc.M109.081562

Christine Bee[‡], Anna Moshnikova[§], Christopher D. Mellor[¶], Justin E. Molloy[¶], Yulia Koryakina[‖], Benjamin Stieglitz[¶1], Andrei Khokhlatchev[§2], and Christian Herrmann[‡]

From the [‡]Department of Chemistry, Physical Chemistry 1, Ruhr-University Bochum, Universitätsstrasse 150, 44780 Bochum, Germany, the Departments of [§]Pathology and [‖]Microbiology, University of Virginia Health Science Center, Charlottesville, Virginia 22908, and the [¶]Medical Research Council National Institute for Medical Research, The Ridgeway, Mill Hill, London NW7 1AA, United Kingdom

NORE1A is a Ras-binding protein that belongs to a group of tumor suppressors known as the Ras association domain family. Their growth- and tumor-suppressive function is assumed to be dependent on association with the microtubule cytoskeleton. However, a detailed understanding of this interplay is still missing. Here, we show that NORE1A directly interacts with tubulin and is capable of nucleating microtubules. Strikingly, the ability to stimulate nucleation is regulated in a dual specific way either via phosphorylation of NORE1A within the Ras-binding domain by Aurora A kinase or via binding to activated Ras. We also demonstrate that NORE1A mediates a negative effect of activated Ras on microtubule nucleation. On the basis of our results, we propose a novel regulatory network composed of the tumor suppressor NORE1A, the mitotic kinase Aurora A, the small GTPase Ras, and the microtubule cytoskeleton.

The small GTPase Ras is defined as a molecular switch that cycles between an inactive GDP-bound and an active GTP-bound conformation (1). In the active form, Ras is able to interact with downstream effectors such as Raf, phosphatidylinositol 3-kinase, and phospholipase Cϵ, which initiate signaling cascades, leading ultimately to vital cellular responses such as transcription, translation, and cell cycle progression (2). The cellular output of a Ras-mediated signal is usually associated with cell growth and proliferation; hence, mutations within the Ras protein are often involved in tumorigenesis (3). Despite the well established function of Ras in cell transformation, there is considerable evidence that Ras can also participate in signaling pathways connected to growth inhibition and tumor suppression. Specifically, a conserved set of polypeptides named the Ras association domain family (RASSF)[3] has been discovered, which bears tumor-suppressive potential (4). The classical RASSF protein family members RASSF1–6 each contain an invariant C-terminal combination of a Ras-binding domain (RBD) followed by a unique coiled-coil region termed the SARAH domain.

Members of the RASSF protein family have been shown to interact with the active form of Ras, which classifies them as *bona fide* Ras effector proteins (5–8). In particular, the complex formation of Ras and RASSF5/NORE1A (novel Ras effector 1A) has been extensively investigated, revealing a high affinity interaction with a dissociation constant in the submicromolar range. The crystal structure of the NORE1 RBD in complex with active Ras has been solved and shows that interaction between the two proteins is established by formation of an intermolecular β-sheet between the switch I region of Ras and strand β_2 of the NORE1 ubiquitin fold. This mode of interaction is similar to previously described structures of complexes between Ras and classical effectors like Raf and guanine nucleotide exchange factors for Ral small GTPases (RalGDS) (9).

Attempts to understand the biological basis for the tumor-suppressive properties of RASSF proteins revealed a common characteristic: their ability to co-localize with the microtubule cytoskeleton. Several reports have shown that individual splice variants of different RASSF members associate with microtubules in the cytoplasm and mitotic spindle. However, endogenous RASSF1A and NORE1A are markedly localized at the centrosome (10, 11). Overexpression, as well as knock-out of RASSF1A, causes a variety of spindle abnormalities (11, 12). These findings give rise to the conclusion that RASSF proteins may carry out an essential function during cell division, maintaining the integrity of the mitotic spindle and thus guaranteeing genomic stability. This feature is likely to contribute to RASSF tumor-suppressive function. A conserved polypeptide stretch of the RASSF proteins has been observed to mediate co-localization with microtubules (10, 11). For RASSF1A, it has also been shown that phosphorylation within this segment by the mitotic kinase Aurora A abolishes microtubule co-localization (13). However, a recent study of Song *et al.* (14) contradicts this finding by showing that RASSF1A phosphorylation by Aurora A might regulate prometaphase progression. Very

* This work was supported by the German National Academic Foundation, the Ruhr University Research School, the Deutsche Forschungsgemeinschaft (SFB 642), the Elsa U. Pardee Foundation, and the CONCERN Foundation.

[S] The on-line version of this article (available at http://www.jbc.org) contains supplemental Figs. S1–S7 and Table S1.

[1] To whom correspondence may be addressed. Tel.: 44-208-816-2059; Fax: 44-208-816-2109; E-mail: bstiegl@nimr.mrc.ac.uk.

[2] To whom correspondence may be addressed. Tel.: 434-982-4967; E-mail: ak9k@cms.mail.virginia.edu.

[3] The abbreviations used are: RASSF, Ras association domain family; RBD, Ras-binding domain; RalGDS, Ral guanine nucleotide dissociation stimulator; GST, glutathione *S*-transferase; PIPES, 1,4-piperazinediethanesulfonic acid; SPR, surface plasmon resonance; TIRF, total internal reflection fluorescence; PKA, protein kinase A; HA, hemagglutinin; siRNA, small interfering RNA; GppNp, guanosine 5′-(β,γ-imido)triphosphate; GpCpp, guanosine 5′-(β,γ-methyleno)triphosphate.

recently, Dallol *et al.* (15) discovered that association of overexpressed RASSF1A with microtubules depends on its interaction with the small GTPase Ran. Aside from these findings, the underlying molecular mechanism of microtubule association is poorly understood. It is still unknown if RASSF members interact directly with tubulin, the building block of the microtubule cytoskeleton. The question of whether RASSF proteins play a role outside of cell division has not been addressed. More importantly, there is no information available addressing the regulatory aspect of RASSF in microtubule dynamics and the role of activated Ras in RASSF functions.

We report here that RASSF5/NORE1A is capable of direct binding to tubulin and inducing microtubule nucleation *in vitro* and in primary human cells. We further show that NORE1A is phosphorylated by the mitotic kinase Aurora A *in vitro* and *in vivo*. The ability of NORE1A to nucleate microtubules is downregulated by Aurora A phosphorylation or by binding of activated Ras. Thus, NORE1A might be a key component in the Ras- and Aurora A-induced regulation of the cellular microtubule network, both receiving signals from those molecules and regulating them.

EXPERIMENTAL PROCEDURES

Mutagenesis and Protein Expression and Purification—All mutants were generated using the QuikChange site-directed mutagenesis kit (Stratagene) according to the manufacturer's instructions and verified by sequencing. The murine NORE1 RBD (amino acids 199–358) and the NORE1 C1-RBD (amino acids 95–358) were expressed as glutathione *S*-transferase (GST) fusion proteins (pGEX vectors, GE Healthcare) in *Escherichia coli* BL21 cells. Proteins were bound to a GSH-Sepharose column (GE Healthcare), cleaved from GST on the column, eluted, and further purified by gel filtration (Superdex 75 column, GE Healthcare) as described (16). In the case of GST-NORE1 RBD, the fusion protein was eluted from the GSH column directly and subjected to gel filtration chromatography. Full-length H-Ras was expressed in *E. coli* CK600K using the pTAC vector. Ras protein was purified essentially as described previously (17). Briefly, the cell lysate was subjected to anion exchange chromatography (DEAE-dextran, GE Healthcare); precipitated with ammonium sulfate; resuspended in 25 mM Tris (pH 7.4), 2.5 mM $MgCl_2$, and 1 mM dithioerythritol; and further purified by gel filtration (Superdex 75 column) in the same buffer. The bound nucleotide was exchanged with GppNp using ammonium sulfate-containing buffer and alkaline phosphatase as described by John *et al.* (18). The identity of Ras and NORE1 constructs was confirmed by mass spectrometry. Tubulin was purified as described previously (19).

Protein Interaction Analysis—GST pulldown assays were performed with 6% CL-glutathione ChroMatrix (Jena Bioscience). The beads were saturated with either GST-NORE1 RBD or the same amount of GST as a control protein. After the initial incubation, beads were washed twice to remove excess protein. Aliquots of the saturated beads were incubated with different concentrations of tubulin under slight agitation (300 rpm) at 10 °C for 1 h in tubulin buffer (80 mM PIPES, 5 mM $MgCl_2$, and 1 mM dithioerythritol, pH 6.6, adjusted with NaOH). The beads were washed once, and bound proteins were eluted with 20 mM GSH in tubulin buffer and analyzed by SDS-PAGE.

For surface plasmon resonance (SPR) measurements, a Biacore 1000 device was used. Unpolymerized tubulin in sodium acetate buffer, pH 3.0, was coupled to a CM5 sensor chip (Biacore) activated with 1-ethyl-3-(3-dimethylaminopropyl)carbodiimide and *N*-hydroxysuccinimide according to the manufacturer's instructions. The remaining free surface was passivated by reaction with ethanolamine. The NORE1 RBD was passed in tubulin buffer through the reference cell and the tubulin-treated flow cell in increasing concentrations at a flow rate of 5 μl/min.

Tubulin polymerization was followed by turbidity measurements at a 350-nm wavelength. 6 μM tubulin in tubulin buffer was mixed quickly with 1 mM GTP and different concentrations of various RBDs. The sample turbidity was recorded in a photometer preheated to 37 °C.

For total internal reflection fluorescence (TIRF) microscopy, the samples were prepared in a flow cell and illuminated by a 488-nm Ar^+ ion laser beam under conditions of total internal reflection as described (20). 5 μM fluorescein-labeled tubulin was polymerized with different concentrations of the NORE1 RBD or control proteins at 37 °C in TIRF buffer (80 mM PIPES, 2 mM $MgCl_2$, and 2 mM EGTA, pH 7, adjusted with KOH). To stabilize microtubules, 1 mM GpCpp (Jena Bioscience) was used. (GpCpp is a GTP analog that is hydrolyzed extremely slowly). At different time points, 1 μl of the sample solution was diluted 1:100 in TIRF buffer and applied to a flow cell. After 5 min of settlement, unbound material was washed out by rinsing with TIRF buffer. For each sample, 10 images were recorded randomly. The length of clearly distinguishable microtubules (approximately from 0.5 μm upwards) was determined using the program GMimPro (21). For every time point, at least 100 microtubules were evaluated.

Phosphorylation of murine NORE1 constructs was tested using recombinant Aurora A (Invitrogen) or protein kinase A (PKA; Biaffin) in phosphorylation buffer (25 mM Tris, 10 mM $MgCl_2$, 1 mM dithiothreitol, 0.5 mM EGTA, 0.5 mM Na_3VO_4, and 0.01% Triton X-100, pH 7.4) containing 100 μM ATP and 5 μCi of [γ-^{32}P]ATP per 25-μl sample volume. Samples were incubated for 30 min at 30 °C with 0.33 mg/liter Aurora A (specific activity of 1.8 μM phosphate transferred per mg/min) or the corresponding amount of PKA. For liquid scintillation counting, 20 μl of each sample was absorbed by phosphocellulose P-81 (Millipore) and washed three times with 0.75% H_3PO_4 and once with acetone. Dried cellulose squares were transferred to scintillation vials with 5 ml of Ultima Gold universal liquid scintillation counting mixture (PerkinElmer Life Sciences) and analyzed with a Tri-Carb 2800 TR scintillation counter (PerkinElmer Life Sciences). For autoradiography, 5 μl of each sample was subjected to SDS-PAGE and analyzed with a FLA-3000 phosphoimager (Fujifilm Life Science). The gels were then stained with Coomassie Blue solution.

The equilibrium dissociation constants of complexes between active Ras and NORE1 RBD variants were determined using the inhibition of guanine nucleotide dissociation upon complex formation. These guanine nucleotide dissociation inhibitor assays were performed as described previously (9).

cDNA Transfection and Immunoprecipitation—Cultivation of human embryonic kidney HEK293 cells (American Type Culture Collection), HEK293 cell transfection, and retroviral supernatant production were performed as described previously (11). HEK293 cells were transfected using Lipofectamine reagent as described previously (6) and harvested 48 h after transfection.

For the detection of NORE1A-Aurora A association, 293 cells were transfected with hemagglutinin (HA)-NORE1A and either FLAG-vector or FLAG-Aurora A kinase. Thirty-six hours later, nocodazole was added to transfected cells. Twelve hours after nocodazole addition, cells were harvested into radioimmune precipitation assay buffer (50 mM Tris-HCl, pH 7.6, 150 mM NaCl, 1% Nonidet P-40, 0.5% sodium deoxycholate, and 0.1% SDS). Lysates were cleared by centrifugation, mixed with anti-FLAG antibodies coupled to Sepharose (Sigma), and incubated at 4 °C for 1.5–2 h. Beads were extensively washed with radioimmune precipitation assay buffer. The precipitates were probed with anti-HA antibody (Covance Inc.) using anti-HA-biotin antibody and avidin-horseradish peroxidase conjugate. Bound antibodies were visualized by ECL (Pierce).

To examine the interaction between full-length NORE1A and Aurora A *in vitro*, 293 cells were transfected separately with the pCMV5-HA vector, HA-Aurora A, or FLAG-NORE1A. Forty-eight hours later, cells were lysed in 30 mM HEPES, pH 7.4, 1% (w/v) Triton X-100, 20 mM β-glycerophosphate, 1 mM orthovanadate, 20 mM NaF, 20 mM KCl, 2 mM EGTA, 7.5 mM $MgCl_2$, 14 mM β-mercaptoethanol, and protease inhibitor mixture (Sigma). HA-expressing lysates were precipitated with anti-HA antibody bound to agarose beads, and the beads were washed. FLAG-NORE1A-expressing lysate was immunoprecipitated with anti-FLAG antibody-agarose; the beads were washed; and NORE1A was eluted from beads using 0.1 mg/ml FLAG-peptide. The eluates were incubated with HA-agarose on which vector or Aurora A was captured for 2 h at 4 °C. After washing, the proteins retained on the beads were subjected to Western blotting with anti-FLAG-biotin antibodies.

Small Interfering RNA (siRNA) Transfection and Immunofluorescence Microscopy—WI-38 primary human fibroblasts (American Type Culture Collection) were propagated according to the manufacturer's instructions. To avoid working with a senescent population, a new stock of WI-38 cells was thawed every 4–5 weeks. The siRNA duplexes against NORE1A (sense strand, 5′-GCAUGAAACUGAGUGAAGAUU-3′, bases 674–694; and sense strand, 5′-UCAAGAAGUUCAUGGUUGUUU-3′, bases 911–931) were purchased from Dharmacon. These two duplexes, duplexes 7 and 8, were the most efficient of four anti-NORE1A duplexes recommended by Dharmacon (supplemental Fig. S7). For transfection, duplexes were mixed at a 1:1 ratio. The control siRNA oligonucleotide was non-targeting siRNA#5 (catalog no. D-001210-005), containing at least four mismatches with all known human genes (Dharmacon). The Alexa Fluor 488-labeled AllStars negative control siRNA (catalog no. 1027284) was from Qiagen (Valencia, CA). The anti-NORE1A siRNA duplexes were mixed with Alexa Fluor-labeled control siRNA at a ratio of 3:1, and the mixture was transfected using DharmaFECT1 reagent (Dharmacon) according to the manufacturer's instructions.

Five to seven days after plating, cells were treated with 10 μg/ml nocodazole in growth medium to depolymerize microtubules. Two hours thereafter, cells were allowed to recover for 1–3 min in fresh medium without nocodazole; treated for 1 min in prewarmed buffer containing 80 mM PIPES-KOH, pH 6.9, 1 mM $MgCl_2$, 1 mM EGTA, 0.5% Triton X-100, and 10% glycerol (22); and fixed in 4% formaldehyde buffered with phosphate-buffered saline for 10 min, followed by permeabilization with 0.2% Triton X-100 buffered with phosphate-buffered saline. The cells were then processed for immunostaining as described (11) with anti-α-tubulin (clone DM1A, Sigma) or anti-NORE1A (clone 10F10) and anti-giantin (catalog no. PRB-114C, Covance Inc.) antibodies. Digital images were taken under UV illumination with appropriate filter sets at ×100 magnification using a Leica DMIRE2 microscope and captured using IPLab 3.6.5a software (Scanalytics, Inc.). Only transfected cells, *i.e.* those containing green dots of siRNA transfection marker, were imaged. To allow comparison of image intensity within each experiment, images for α-tubulin and giantin were processed identically in the Adobe Photoshop program.

SYBR Green Real-time Quantitative Reverse Transcription-PCR—Total cellular RNA from WI-38 cells transfected with siRNA duplexes as described above was extracted using an RNeasy mini kit coupled with an RNase-free DNase set (Qiagen). Two micrograms of total RNA was reverse-transcribed using an iScript cDNA synthesis kit (Bio-Rad).

Real-time quantitative reverse transcription-PCR analysis of NORE1A mRNA for detection of NORE1A knockdown was performed using the CFX96™ real-time PCR detection system and software (Bio-Rad). NORE1A primers were designed using Beacon Designer software (Premier Biosoft International). The primers used are as follows: NORE, 5′-GCTGCTCAAGAAGTTCAT-3′ (forward) and 5′-TTGTCCGTCCTTGTGTAT-3′ (reverse); and PSMB6, 5′-CAAACTGCACGGCCATGATA-3′ (forward) and 5′-GAGGCATTCACTCCAGACTGG (reverse). The PSMB6 proteasomal subunit mRNA was used as a reference.

Real-time reverse transcription-PCR was performed with the SYBR Green Supermix (Bio-Rad) using 2 μl of cDNA and 300 nmol/liter primers in a total volume of 20 μl in triplicates. PCR conditions were 95 °C for 3 min, followed by 40 cycles consisting of 15 s at 95 °C, 30 s at 58.7 °C, and 30 s at 72 °C for NORE1A and 95 °C for 3 min, followed by 40 cycles consisting of 15 s at 95 °C, 30 s at 62 °C, and 30 s at 72 °C for PSMB6.

Relative expression levels of target sequences were determined by the standard curve method using cDNA from the WI-38 cell line overexpressing NORE1A, which was serially diluted 10-fold (100 to 0.01 ng). Expression levels of NORE1A were normalized to PSMB6 levels.

RESULTS

The NORE1 RBD Forms a Complex with α/β-Tubulin in Vitro—The NORE1 RBD consists of a total of 160 amino acids and is nearly twice as large as classical RBDs, such as found in Raf and RalGDS. Strikingly, cell biological studies have shown that exactly this 160-amino acid stretch that forms the RBD is necessary to observe a co-localization of NORE1 and microtubules (11). This observation prompted us to examine whether

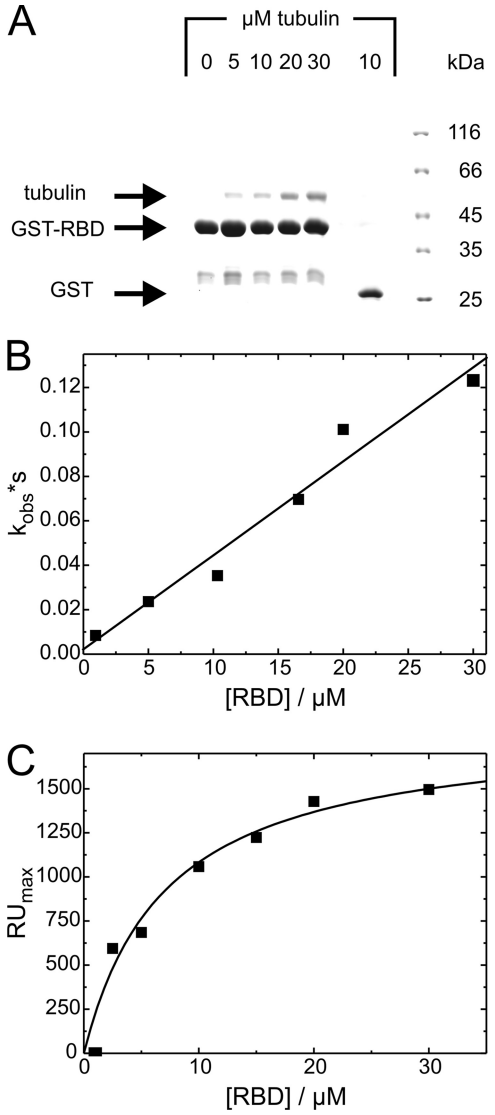

FIGURE 1. **Direct interaction of the NORE1 RBD with tubulin.** *A*, pulldown of tubulin with GST-NORE1 RBD. GSH beads were saturated with GST-NORE1 RBD or GST and incubated with various concentrations of tubulin. Eluates were analyzed by SDS-PAGE. *B*, determination of the association rate constant for SPR measurements of NORE1 RBD association and dissociation on immobilized tubulin. *C*, plotting the maximum shift of the resonance angle (RU_{max}) against concentration leads to a hyperbolic binding curve.

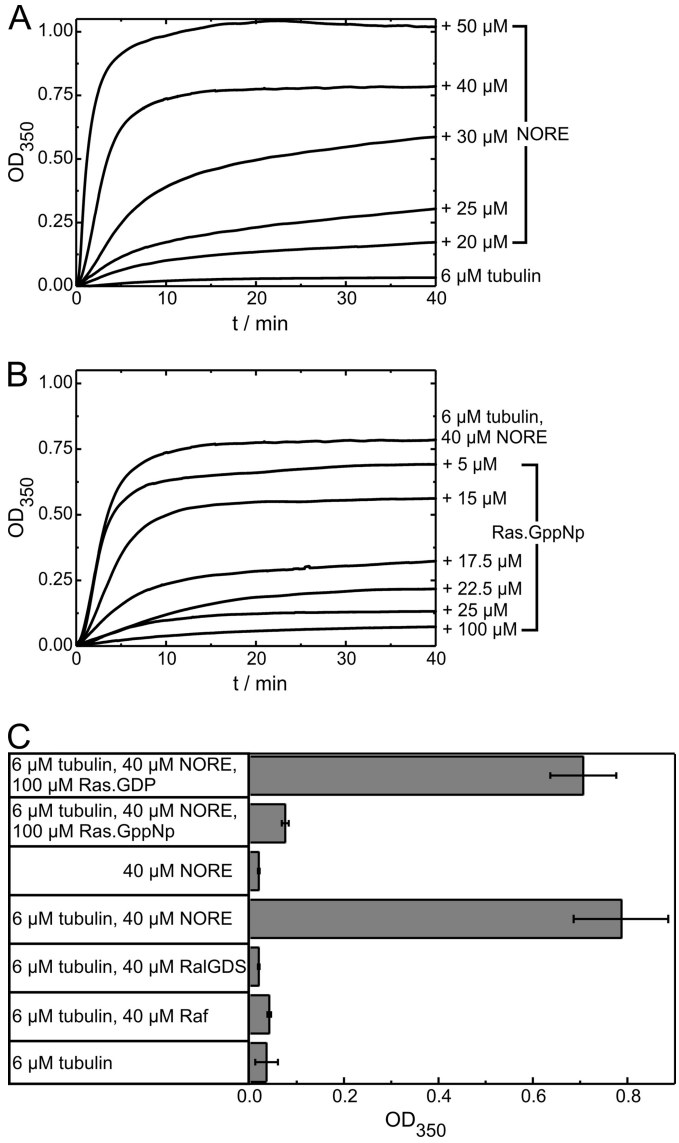

FIGURE 2. **Tubulin polymerization followed by turbidity.** 6 μM tubulin was incubated with 1 mM GTP at 37 °C and various concentrations of the NORE1 RBD alone (*A*), the NORE1 RBD and activated Ras (*B*), or control RBDs (*C*). The absorbance was detected at 350 nm. *Error bars* indicate the variation in turbidity of each experiment, which was performed at least three times.

the RBD of NORE1 is capable of binding directly with tubulin *in vitro*. We performed GST pulldown assays to investigate a potential interaction between the NORE1 RBD and tubulin. Using bacterially expressed GST-NORE1 RBD and purified pig brain tubulin, we detected a direct interaction between both proteins (Fig. 1*A*). The assay was performed in the absence of GTP at 10 °C and at a tubulin concentration range of 5–30 μM. Under these conditions, α/β-tubulin does not form microtubules, and thus, the interaction determined in the pulldown assay is a binding event between unpolymerized α/β-tubulin dimers and the NORE1 RBD. To investigate this interaction in a quantitative manner, we used SPR spectroscopy. Unpolymerized tubulin was immobilized by standard 1-ethyl-3-(3-dimethylaminopropyl)carbodiimide coupling on a Biacore CM5 chip matrix, and increasing amounts of the NORE1 RBD were injected. Analysis of the SPR response showed an association rate constant of 4000 M^{-1} s^{-1} (Fig. 1*B*) and a dissociation rate constant of 0.055 s^{-1}. An equilibrium dissociation constant of $K_d = 10 \pm 5$ μM was calculated from both the kinetic values and the maximal SPR response (Fig. 1*C*). These results demonstrate that the RBD of NORE1 alone is able to directly interact with α/β-tubulin dimers *in vitro*.

NORE1A Stimulates Tubulin Nucleation in the Absence of Active Ras—Having determined a direct interaction between the NORE1 RBD and tubulin, we hypothesized a regulatory impact of NORE1A on microtubule formation. We therefore investigated the effects of the NORE1 RBD on microtubule assembly *in vitro*. Polymerization of pure pig brain tubulin was followed by an increase in sample turbidity at a 350-nm wavelength. Under our experimental conditions, 6 μM α/β-tubulin alone did not assemble markedly into microtubules. However, the addition of the NORE1 RBD resulted in a concentration-dependent turbidity increase,

indicating the induction of microtubule assembly (Fig. 2*A*). Remarkably, the addition of active GppNp (a non-hydrolyzable GTP analog)-loaded Ras markedly impeded this effect in a dose-dependent manner (Fig. 2*B*). To further prove the specificity of the NORE1 RBD-induced turbidity increase, we performed the turbidity assay using the RBDs of Raf kinase and RalGDS as a control. We did not observe any significant increase in turbidity (Fig. 2*C*) with either of these control proteins.

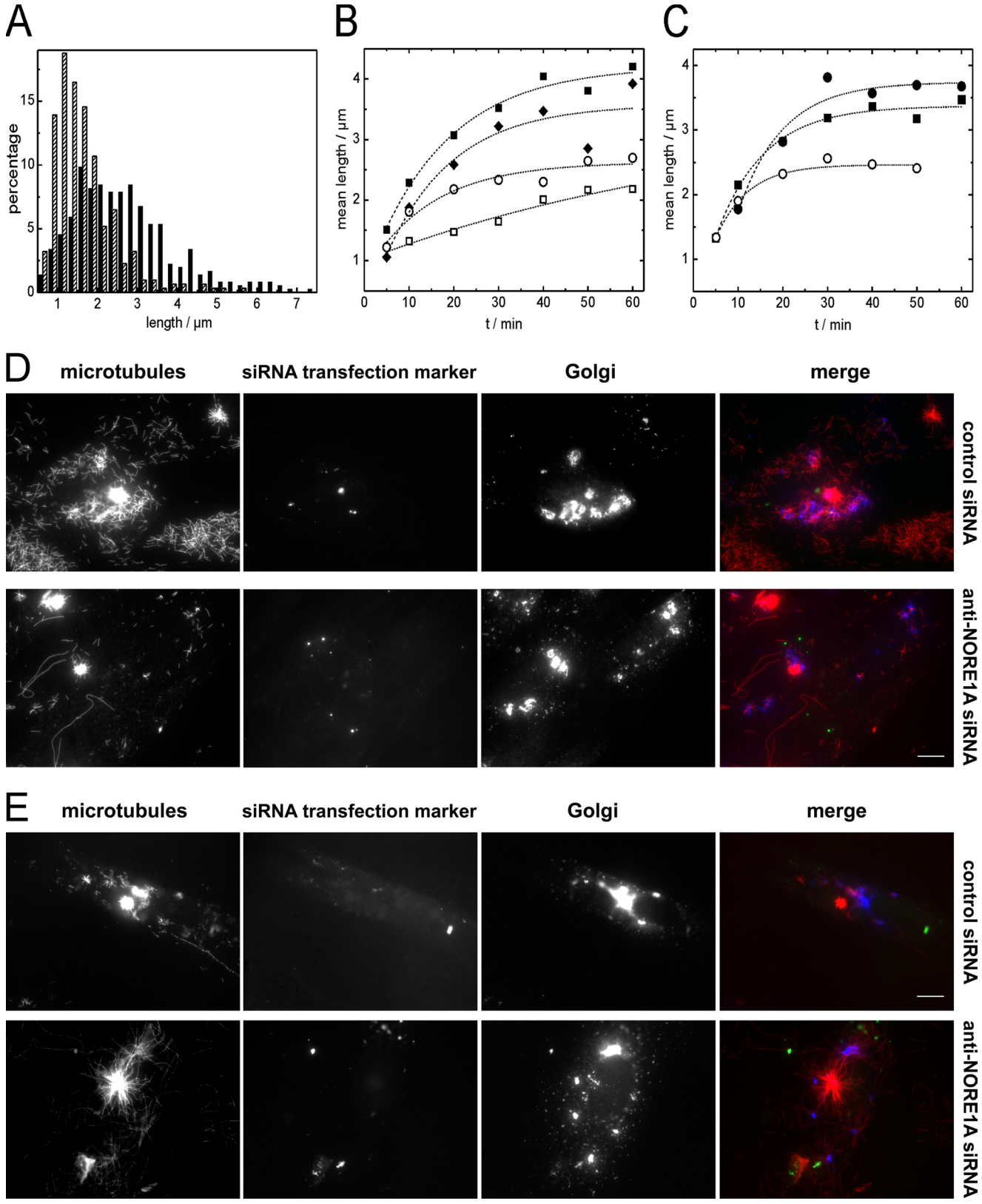

To determine the mechanism behind the enhanced turbidity, we used TIRF microscopy to visualize the morphology of NORE1 RBD-induced microtubules. Pure fluorescein-labeled α/β-tubulin that was incubated with the slowly hydrolyzable GTP analog GpCpp produced single microtubules with an average size of 3.5 μm after 30 min of incubation at 37 °C. Remarkably, the addition of 60 μM NORE1 RBD led to much shorter microtubules with an average size of 1.6 μm and a narrower size distribution (Fig. 3*A*). The reduction of microtubule length was concentration-dependent (Fig. 3*B*) and specific for the NORE1 RBD. The addition of the RalGDS RBD did not induce any alterations in microtubule length or dynamics compared with tubulin alone (supplemental Fig. S1). Interestingly, the addition of active Ras abolished the effect of the NORE1 RBD on microtubule length (Fig. 3*C*). Whereas the length was drastically reduced in the presence of the NORE1 RBD, there was no alteration in microtubule shape or bundling observed (supplemental Fig. S2). Taken together, the induction of tubulin polymerization, increased turbidity, and reduction of individual microtubule lengths, these results indicate that NORE1A is involved in microtubule nucleation. If NORE1A creates more polymerization nuclei, the fraction of polymerized tubulin increases faster, and a higher sample turbidity is measured. Under these conditions, more growing polymers compete for a limited amount of monomers, and thus, the resulting polymers are shorter than in the absence of NORE1A. This nucleation effect is mediated by the NORE1 RBD and can be regulated by Ras.

To determine whether full-length NORE1A is involved in the regulation of microtubule nucleation *in vivo*, we depleted NORE1A by RNA interference in WI-38 primary human fibroblasts, depolymerized microtubules with nocodazole, and examined microtubule nucleation after nocodazole washout. Quantification of the siRNA-mediated depletion by quantitative reverse transcription-PCR revealed that, under the experimental conditions used, the NORE1A message was reduced by 3.1-fold (supplemental Fig. S3). Fig. 3*D* shows that NORE1A depletion markedly reduced microtubule nucleation by noncentrosome sources, specifically the Golgi vesicles.

The expression of activated H-Ras in WI-38 cells suppressed microtubule nucleation after nocodazole washout (Fig. 3*E*, *upper row*). Interestingly, if NORE1A was depleted in WI-38 cells expressing activated H-Ras, the negative effect of Ras on microtubule nucleation was strongly attenuated (Fig. 3*E*, *lower row*). The amount of activated H-Ras expressed in WI-38 cells was not affected by NORE1A siRNA depletion (supplemental Fig. S4). These data suggest that the Ras-induced negative effect on microtubule nucleation is at least in part mediated by NORE1A.

NORE1A Interacts with Aurora A Kinase—It has been reported recently that RASSF1A interacts with Aurora A *in vitro* and in transfected cells (13, 14, 23). We have found that NORE1A is also capable of interacting with Aurora A kinase in transfected 293 cells (Fig. 4*A*). NORE1A and Aurora A also interact *in vitro*. As shown in Fig. 4*B*, Aurora A and NORE1A proteins, immunopurified from 293 cells, are capable of forming a complex *in vitro*. Thus, Aurora A and NORE1A are capable of interaction both *in vitro* and *in vivo*.

The NORE1 RBD Is Phosphorylated by Aurora A—Rong *et al.* (13) reported RASSF1A phosphorylation by Aurora A at Thr^{202} and/or Ser^{203}. Mimicking phosphorylation by mutating these two residues to glutamate abolished binding to microtubules and RASSF1-induced M phase cell cycle arrest. As the phosphorylation site is conserved in the NORE1 RBD, we examined whether phosphorylation by Aurora A is a regulatory mechanism for NORE1-tubulin interactions. We subjected different NORE1A constructs to *in vitro* phosphorylation by recombinant Aurora A and analyzed the samples by liquid chromatography/tandem mass spectrometry. Full-length human NORE1A, which was immunoprecipitated from transfected cells, was phosphorylated mainly at Ser^{277} (supplemental Table S1). Thr^{276} was phosphorylated to a much lesser extent (data not shown). Ser^{277} of human NORE1A corresponds to Ser^{203} of RASSF1 and Ser^{274} or murine NORE1. We further tested the purified recombinant murine NORE1 RBD and the N-terminally elongated NORE1 C1-RBD (amino acids 95–358) construct in the *in vitro* phosphorylation assay. Ser^{274} was identified as the only effective Aurora A phosphorylation site in both constructs (data not shown).

In cotransfection experiments, a kinase-dead mutant of Aurora A, D274A, was capable of interacting with NORE1A much more efficiently than wild-type Aurora A (supplemental Fig. S5), suggesting that NORE1A dissociates from Aurora A upon phosphorylation. Such behavior is common for substrates of other kinases and has been suggested to occur in the case of the Aurora A substrate HEF1 (24).

To further investigate Aurora A-dependent phosphorylation, we used the recombinant NORE1 RBD in the *in vitro* kinase assay in the presence of [γ-^{32}P]ATP. Fig. 4*C* shows that the NORE1 RBD could be selectively phosphorylated by Aurora A. The RalGDS RBD, used as a control for Aurora A substrate specificity, was not phosphorylated. As an additional control, we used PKA, a kinase with virtually the same consensus sequence as Aurora A (25). Although the NORE1 RBD corre-

FIGURE 3. **Size distribution of tubulin polymers investigated by TIRF microscopy and tubulin nucleation *in vivo*.** *A*, shown are histograms of microtubules after 30 min of incubation of tubulin under polymerization conditions. *Black bars*, pure tubulin; *hatched bars*, tubulin with 60 μM NORE1 RBD. *B*, shown is the mean microtubule length as a function of time and NORE1 RBD concentration. ■, pure tubulin; ♦, 15 μM NORE1 RBD; ○, 30 μM NORE1 RBD; □, 60 μM NORE1 RBD. *C*, shown is a time course with pure tubulin (■), 30 μM NORE1 RBD (○), and 30 μM NORE1 RBD + 60 μM Ras-GppNp (●). *Lines* are guides to the eye. *D* and *E*, WI-38 cells were transfected with anti-NORE1A siRNA duplexes or control siRNA both containing Alexa Fluor 488-labeled control siRNA marker. In *E*, cells were infected with retrovirus encoding the G12V H-Ras oncoprotein 2 days later. Seven days (*D*) or 6 days (*E*) post-transfection, cellular microtubules were depolymerized with nocodazole, recovered for 1.5 min (*D*) or 2 min (*E*) in nocodazole-free medium, and processed as described under "Experimental Procedures." Transfection marker-positive cells were processed for immunofluorescence and imaged as described. Shown are microtubules (stained with α-tubulin), the siRNA transfection marker, the Golgi (stained with giantin), and a superimposed image (*red*, tubulin; *green*, siRNA marker; *blue*, giantin). *Scale bar* = 10 μm (refers to all panels). The experiments were performed three times with similar results, and representative data are shown. Similar effects of NORE1A and Ras on microtubule nucleation were seen if cells were assayed 5 days after transfection or if the nocodazole recovery was carried out for 2–2.5 min. The infection efficiency of the Ras-encoding retrovirus was 80–90% based on flow cytometry assay.

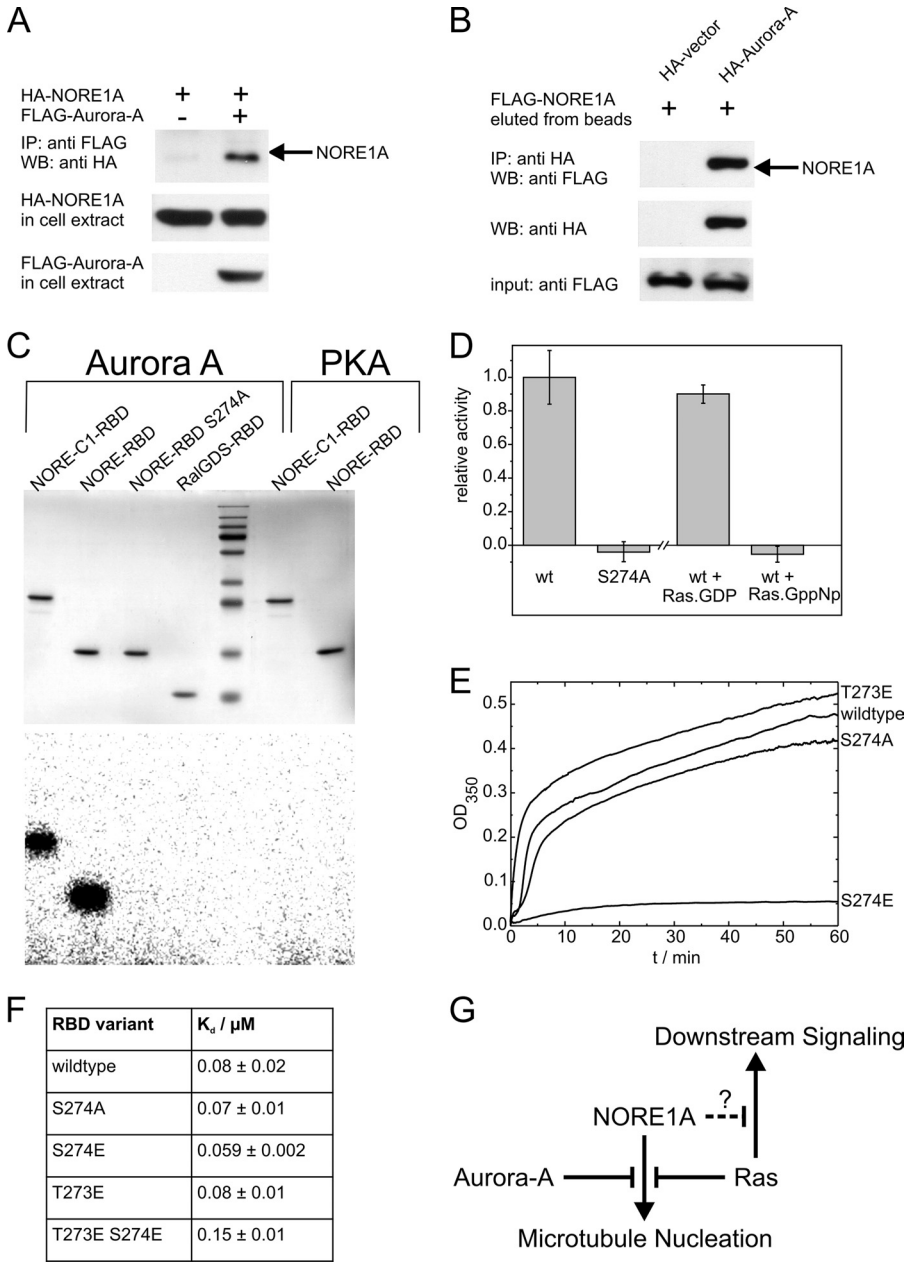

RBD variant	K_d / μM
wildtype	0.08 ± 0.02
S274A	0.07 ± 0.01
S274E	0.059 ± 0.002
T273E	0.08 ± 0.01
T273E S274E	0.15 ± 0.01

FIGURE 4. **Phosphorylation of NORE1A by Aurora A and interaction of NORE1 phosphorylation site mutants with tubulin and activated Ras.** *A*, 293 cells were transfected with cDNAs as indicated. Thirty-six hours later, nocodazole was added to transfected cells. Twelve hours later, cells were lysed, and lysates were subjected to immunoprecipitation (*IP*) or probed as indicated. A representative experiment of three is shown. *B*, 293 cells were transfected separately with the pCMV5-HA vector, HA-Aurora A, or FLAG-NORE1A. HA- and FLAG-tagged proteins were purified from cells and subjected to *in vitro* interaction assay as described under "Experimental Procedures." The *upper panel* shows a Western blot (*WB*) of proteins retained on HA beads after the interaction assay. A representative experiment of three is shown. *C*, 10 μM solutions of different murine NORE1 constructs and the RalGDS RBD were incubated with [γ-^{32}P]ATP and Aurora A or PKA as a control kinase. Samples were analyzed by SDS-PAGE (*upper panel*) and phosphoimaging (*lower panel*). *D*, 10 μM solutions of NORE1 RBD constructs with or without Ras-GDP or Ras-GppNp (20 μM each) were incubated with Aurora A in the presence of [γ-^{32}P]ATP, and samples were subjected to liquid scintillation counting. *Error bars* show the maximal deviation based on three independent measurements. *wt*, wild-type. *E*, 6 μM tubulin was incubated with 1 mM GTP and different NORE1 RBD variants (30 μM). *F*, equilibrium dissociation constants (K_d) for complexes between murine NORE1 RBD variants and H-Ras were determined by guanine nucleotide dissociation inhibitor assays. *G*, shown is NORE1A as regulatory node of microtubule formation activity controlled by two distinct inputs, activated Ras and Aurora A kinase.

sponds to this sequence, it was not phosphorylated by PKA (Fig. 4*C*, *last two lanes*). An S274A mutant of the NORE1 RBD was not phosphorylated by Aurora A, further confirming that the NORE1 RBD is exclusively phosphorylated at Ser^{274}.

The addition of active GppNp-loaded Ras completely inhibited NORE1 RBD phosphorylation by Aurora A, whereas inactive Ras-GDP did not have any effect on phosphorylation (Fig. 4*D*). These data suggest that interactions with active Ras protect the NORE1 RBD from phosphorylation by Aurora A.

The NORE1 RBD S274E Phosphomimetic Mutant Fails to Induce Tubulin Polymerization, whereas the Interaction with Ras Is Conserved—To mimic phosphorylation and to investigate its effects, we introduced glutamate residues into the NORE1 RBD and tested the ability of different mutants to induce tubulin polymerization in turbidity assays (Fig. 4*E*). The introduction of a negative charge at position 274 (NORE1 RBD S274E mutant) was sufficient to suppress NORE1 RBD-induced tubulin polymerization completely. Strikingly, neither mutation of the adjacent residue (T273E) nor mutation of Ser^{274} to alanine significantly reduced polymerization efficacy (Fig. 4*E*). Mutating Thr^{273} to Glu in addition to the S274E mutation did not result in an increased effect (supplemental Fig. S6). Interestingly, the affinity of the NORE1 RBD for H-Ras *in vitro* was not affected by the T273E, S274E, or S274A mutation and was only slightly affected by the T273E/S274E double mutation (Fig. 4*F*). Phosphorylation at Ser^{274} therefore seems to be a specific mechanism for regulation of NORE1-induced tubulin nucleation and polymerization.

DISCUSSION

The growth and putative tumor suppressor NORE1A is a RASSF member and has been originally identified as a Ras effector. In contrast to other effector proteins, NORE1A lacks any catalytic activity, and it is assumed to function as an adaptor that recruits other signaling components. Many independent reports have shown that RASSF proteins co-localize with microtubular structures. Nevertheless, it is still uncertain if association with the microtubule cytoskeleton is a functional prerequisite for the growth- and tumor-suppressive function of the RASSF protein. Here, we

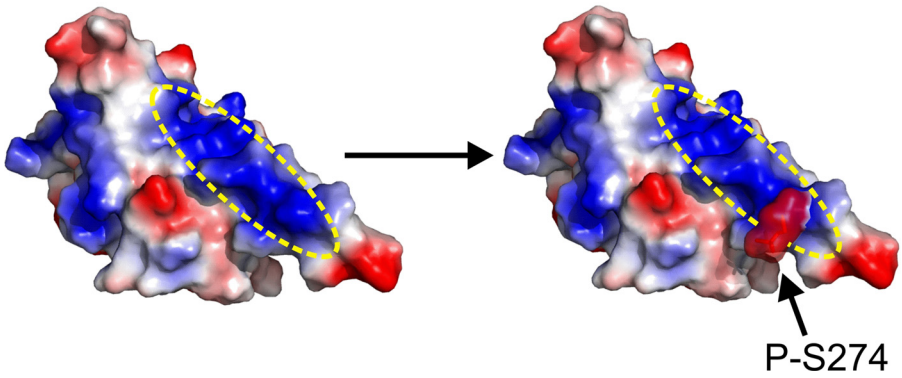

FIGURE 5. **Surface variation of the electrostatic potential of the NORE1 RBD upon phosphorylation by Aurora A.** Shown is a surface presentation of the NORE1 RBD (Protein Data Bank code 3DDC) with the electrostatic potential before and after phosphorylation at Ser^{274}. the color code is *blue* for positive charges, *red* for negative charges, and *white* for neutral surface. The positive charged patch suitable for electrostatic interaction with tubulin is indicated. This figure was generated using PyMOL.

have investigated the underlying mechanism of RASSF-microtubule co-localization, and we have revealed a novel regulatory role of the RASSF member NORE1A.

We have shown that the NORE1 RBD directly binds tubulin and is capable of nucleating tubulin polymerization *in vitro* without further scaffold proteins or other interaction partners. Most importantly, the microtubule-nucleating competence of the NORE1 RBD is repressed upon binding to active GTP-loaded Ras, suggesting that Ras is able to regulate microtubule formation via NORE1A. Validation of these results under *in vivo* conditions has revealed that NORE1A is indeed involved in microtubule nucleation. When endogenous NORE1A was depleted in primary human fibroblasts, the number of microtubules nucleated at cytoplasmic sources, specifically at Golgi vesicles, was drastically reduced. Strikingly, the same effect was obtained by overexpression of oncogenic Ras. In line with our *in vitro* data, these findings indicate that Ras activation leads to inhibition of NORE1A-induced microtubule nucleation. This might be the mechanism connecting Ras-NORE1A interaction with growth and tumor suppression.

The dynamics of complex formation between active Ras and NORE1A strongly differs from that of other Ras-effector complexes. In particular, the lifetime of the Ras-NORE1A complex is 100–1000 times longer than that of any other Ras-effector complex (9). This notable feature could be beneficial for effective sequestration of NORE1A, preventing it from inducing microtubule nucleation. Interestingly, if NORE1A is depleted in primary human fibroblasts that simultaneously overexpress oncogenic Ras, the nucleation of cytoplasmic microtubules is partially recovered. This rescue phenotype may be explained by interference with a signaling pathway that becomes dominant under conditions of both overexpression of oncogenic Ras and down-regulation of the tumor suppressor NORE1A. However, the mechanism causing this reverse phenotype needs to be addressed by further investigations.

The regulation of microtubule nucleation via NORE1A is not exclusively dependent on Ras. We have shown that NORE1A is a binding partner and substrate of the mitotic kinase Aurora A. Strikingly, we demonstrated that Aurora A-directed phosphorylation at Ser^{274} within the RBD of NORE1A results in impairment of its microtubule-nucleating ability. Thus, our data suggest that the growth and putative tumor suppressor NORE1A is a regulator of microtubule formation activity that is controlled by two distinct inputs, activated Ras and Aurora A kinase (Fig. 4*G*).

The crystal structure of the NORE1 RBD shows that the Aurora A phosphorylation site is located outside the Ras-NORE1A interface. Interestingly, the electrostatic potential of the NORE1 RBD indicates that Ser^{274} is part of a large positively charged patch. Several known microtubule-associated proteins have been reported to form electrostatic interactions with the acidic C terminus of tubulin (26). If NORE1A and tubulin interact in a similar manner, it is likely that introduction of two negative charges due to phosphorylation will disturb the electrostatics-based interaction of tubulin and NORE1A (Fig. 5).

Because the Aurora A phosphorylation site is not located within the interface of the Ras-NORE1A complex, it is not surprising that phosphorylation does not affect the interaction between Ras and NORE1A. However, we clearly showed that Aurora A is not capable of phosphorylating NORE1A in the presence of active Ras. This might be explained by the interaction of both Ras and Aurora A with overlapping regions of the NORE1 RBD. Alternatively, Ras might alter NORE1A conformation, restricting access of Aurora A kinase to phosphorylation sites.

It is a remarkable observation that interactions of NORE1A with Aurora A, tubulin, and Ras are all mediated by overlapping sections of one and the same NORE1A module, the RBD. The RBDs of Raf, phospholipase Cϵ, and RalGDS, which are rather rigid binding units, are known to interact exclusively with the active form of Ras. In contrast, the RBD of NORE1 functions as an integrative platform for various binding partners that can be modulated by phosphorylation. In comparison with the classical counterparts, it is extended at the N terminus by an α-helix and by a loop insertion between strands β_1 and β_2 that harbors the phosphorylation site. It seems likely that the extended size is responsible for the functional diversity of the NORE1 RBD beyond mere Ras binding.

The members of the RASSF protein family share the same domain architecture with significant sequence homology. NORE1A in particular shares significant homology with RASSF1 and RASSF3. Similar to NORE1A, association with the microtubule cytoskeleton has been described for both proteins. Furthermore, RASSF1 undergoes phosphorylation by Aurora A at a position homologous to Ser^{277} in human NORE1A (13). These similarities suggest that the Ras association domains of other RASSF proteins might also function as scaffolds capable of integrating different cellular processes such as signaling via Aurora A or Ras and modulating the microtubular cytoskeleton.

Acknowledgment—We thank Juergen Kuhlmann for help with SPR spectroscopy.

REFERENCES

1. Vetter, I. R., and Wittinghofer, A. (2001) *Science* **294,** 1299–1304
2. Malumbres, M., and Barbacid, M. (2003) *Nat. Rev. Cancer* **3,** 459–465
3. Downward, J. (2003) *Nat. Rev. Cancer* **3,** 11–22
4. van der Weyden, L., and Adams, D. J. (2007) *Biochim. Biophys. Acta* **1776,** 58–85
5. Vavvas, D., Li, X., Avruch, J., and Zhang, X. F. (1998) *J. Biol. Chem.* **273,** 5439–5442
6. Khokhlatchev, A., Rabizadeh, S., Xavier, R., Nedwidek, M., Chen, T., Zhang, X. F., Seed, B., and Avruch, J. (2002) *Curr. Biol.* **12,** 253–265
7. Vos, M. D., Martinez, A., Ellis, C. A., Vallecorsa, T., and Clark, G. J. (2003) *J. Biol. Chem.* **278,** 21938–21943
8. Eckfeld, K., Hesson, L., Vos, M. D., Bieche, I., Latif, F., and Clark, G. J. (2004) *Cancer Res.* **64,** 8688–8693
9. Stieglitz, B., Bee, C., Schwarz, D., Yildiz, O., Moshnikova, A., Khokhlatchev, A., and Herrmann, C. (2008) *EMBO J.* **27,** 1995–2005
10. Liu, L., Tommasi, S., Lee, D. H., Dammann, R., and Pfeifer, G. P. (2003) *Oncogene* **22,** 8125–8136
11. Moshnikova, A., Frye, J., Shay, J. W., Minna, J. D., and Khokhlatchev, A. V. (2006) *J. Biol. Chem.* **281,** 8143–8152
12. Guo, C., Tommasi, S., Liu, L., Yee, J. K., Dammann, R., and Pfeifer, G. P. (2007) *Curr. Biol.* **17,** 700–705
13. Rong, R., Jiang, L., Sheikh, M., and Huang, Y. (2007) *Oncogene* **26,** 8657–8664
14. Song, S. J., Song, M. S., Kim, S. J., Kim, S. Y., Kwon, S. H., Kim, J. G., Calvisi, D. F., Kang, D., and Lim, D. S. (2009) *Cancer Res.* **69,** 2314–2323
15. Dallol, A., Hesson, L. B., Matallanas, D., Cooper, W. N., O'Neill, E., Maher, E. R., Kolch, W., and Latif, F. (2009) *Curr. Biol.* **19,** 1227–1232
16. Wohlgemuth, S., Kiel, C., Krämer, A., Serrano, L., Wittinghofer, F., and Herrmann, C. (2005) *J. Mol. Biol.* **348,** 741–758
17. Tucker, J., Sczakiel, G., Feuerstein, J., John, J., Goody, R. S., and Wittinghofer, A. (1986) *EMBO J.* **5,** 1351–1358
18. John, J., Sohmen, R., Feuerstein, J., Linke, R., Wittinghofer, A., and Goody, R. S. (1990) *Biochemistry* **29,** 6058–6065
19. Waterman-Storer, C. M. (2001) *Curr. Protoc. Cell Biol.* Chapter 13, Unit 13.1
20. Mashanov, G. I., Tacon, D., Knight, A. E., Peckham, M., and Molloy, J. E. (2003) *Methods* **29,** 142–152
21. Mashanov, G. I., and Molloy, J. E. (2007) *Biophys. J.* **92,** 2199–2211
22. Lieuvin, A., Labbé, J. C., Dorée, M., and Job, D. (1994) *J. Cell Biol.* **124,** 985–996
23. Liu, L., Guo, C., Dammann, R., Tommasi, S., and Pfeifer, G. P. (2008) *Oncogene* **27,** 6175–6186
24. Pugacheva, E. N., and Golemis, E. A. (2005) *Nat. Cell Biol.* **7,** 937–946
25. Songyang, Z., Blechner, S., Hoagland, N., Hoekstra, M. F., Piwnica-Worms, H., and Cantley, L. C. (1994) *Curr. Biol.* **4,** 973–982
26. Downing, K. H. (2000) *Annu. Rev. Cell Dev. Biol.* **16,** 89–111